Article

An Influence of Structural Parameters of Nanoporous Alumina Matrices on Optical Properties

Ekaterina Muratova , Alina Ponomareva [*] , Andrey Shemuhin , Yuriy Balakshin , Aleksandr Evseev , Vyacheslav Moshnikov , Anton Zhilenkov , Olga Kichigina [*]

Article

An Influence of Structural Parameters of Nanoporous Alumina Matrices on Optical Properties

Ekaterina N. Muratova [1,2,*]**, Alina A. Ponomareva** [3,4,*]**, Andrey A. Shemukhin** [5,*]**,**
Yuriy V. Balakshin [5]**, Aleksandr P. Evseev** [5,6]**, Vyacheslav A. Moshnikov** [1]**, Anton A. Zhilenkov** [2]
and Olga Yu. Kichigina [2]

[1] Department of Micro- and nanoelectronics, Saint Petersburg Electrotechnical University "LETI", ul. Prof. Popova 5, 197376, Saint Petersburg, Russia

[2] Department of Cyber-phisical Systems, Saint Petersburg Marine Technical University "SMTU", Leninsky pr. 101, 198303, Saint Petersburg, Russia

[3] Center of chemical engineering, Saint-Petersburg National Research University of Information Technologies Mechanics, and Optics (ITMO University), Kronverksky Pr. 49, 197101, Saint Petersburg, Russia

[4] Polytechnical Institute, Far Eastern Federal University (FEFU), 10 Ajax Bay, Russky Island, 690922, Vladivostok, Russia

[5] Skobeltsyn Institute of Nuclear Physics, Moscow State University, Leninskie gory 1(2), 119991, Moscow, Russia

[6] Faculty of Physics, Moscow State University, Leninskie gory1(2), 119991, Moscow, Russia

[*] Correspondence: sokolovaeknik@yandex.ru (E.N.M.); ap_k@inbox.ru (A.A.P.); shemuhin@gmail.com (A.A.S.)

Abstract: In this work, two types of nanoporous alumina membranes were prepared using different acids and were tested. Structural features of the samples were investigated by scanning electron spectroscopy and further by different types of fractal dimension estimation methods. Transmission and scattering of accelerated He+ ions were studied in experiments on ion irradiation of dielectric channels based on porous alumina. Ion accelerator was used as a source of the He+ beam with an energy of 1.7 MeV. A scattering of ions was studied by Rutherford backscattering spectrometry. Helium transition through nanoporous alumina at various angles between the normal to the sample and the beam direction were observed. It is shown that the porous structure of anodic aluminum oxide is excellent as a dielectric matrix of nanocapillaries. Owing to the small angle scattering, it allows the transportation of the accelerated charged particles through the dielectric capillaries, and, as a result, localization of high energy ion irradiation effects. Additionally, according to the transmission UV-Vis spectra the energy gaps of samples obtained were calculated.

Keywords: localized radiation effects; nanoporous alumina; membranes; ion beams; Rutherford backscattering; surface structure; optical properties

1. Introduction

Synthesis, study of nanomaterials and consideration of new areas of their application are increasingly attracting the attention of scientists from different countries (Ahmad et al. 2022, Saad et al. 2021, Hamad et al. 2019). The topic of positive ions passing through a dielectric channel began to be intensively studied in the 1990s since the discovery of guiding effect. For many applications materials with capillaries or porous membranes, that can be used as focusing devices, are interesting from the standpoint of their transmissive properties, a crucial objective being the dependence of the ion transmission coefficient on the incidence angle of the beam. Authors (Stolterfoht and Yamazaki 2016, Borka et al. 2017, Pinilla et al.2019) have shown that a dielectric channel is possibly to form mechanically or by chemical etching. In addition, the publications are considered with structures

based on porous alumina (Su et al. 2018, Costa et al. 2019, Liu et al. 2020) and silicon (Evseev et al. 2020) and other (Bensaid et al. 2018, Abdel-Zaher et al. 2017) as promising materials in the field of sensing, separation of chemicals and compounds, where the properties of the devices being created depend significantly on the pore parameters.

In (Stolterfoht et al. 2002), the transition of multiply charged Ne^{7+} ion beams with an energy of 3 keV through dielectric nanocapillaries in a PET film with a thickness of 10 μm was considered. It was found that the output current was observed even at large angles of inclination of the sample relative to the beam axis, and most of the ions maintained their charge state, the experiment was repeated using different types of ions in a wide range of energies and different nanocapillary structures. It was shown that the charge state of the incident ions affects the angular distribution of the ions passed through capillary. In the case of the beam co-direction and the capillary axis, the shape of the angular distributions for different charge states was identical.

The focusing coefficient is defined as the ratio of the densities of the input and output currents. It depends on the type and energy of the ions and the shape of the capillary. This coefficient varies in a wide range from 10 for Ar^{8+} with an energy of 8 keV to 1000 for He^+ with an energy of 2 MeV. Studies (Du et al. 2015, Fujita et al. 2011, Folkard et al. 2009, Grotzer et al. 2015, Michelet et al. 1999) showed that dielectric micro- and nanocapillary structures have great potential for solving a large number of applied problems, such as bringing an ion beam to air for microelement analysis of particle-induced X-ray emission (PIXE) and Rutherford backscattering spectrometry (RBS) methods, local microelement analysis, micro- and nanolithography and irradiation of biological objects.

Regarding alumina oxide with porous structure were conducted some amount of works associated with beam transition and the change of its parameters at the output. Much attention was paid to the influence of the porous structure parameters on the outgoing beam properties. Nanoporous alumina matrices, also known as porous anodic alumina (PAA), are widely studied for their unique optical properties by Feng and Ji 2021, Domagalski et al. 2021, Ruiz-Clavijo et al. 2021, Davoodi et al. 2020, Alvarez-Carrizal et al. 2021, Pandey et al. 2016. The structural parameters of these matrices can significantly influence their optical characteristics. Understanding and controlling these structural parameters in nanoporous alumina matrices allow researchers to engineer their optical properties for various applications, including photonic devices, sensors, optical filters, and photovoltaics, among others. It is important to note that specific experimental techniques and fabrication processes can influence the optical properties of nanoporous alumina matrices, and further research in this field is ongoing to explore novel optical phenomena and applications.

Authors (Vokhmyanina et al. 2013, Zhang et al. 2016, Röding et al. 2022) have demonstrated that while passing through a dielectric channel positive ions can interact with the channel material and undergo various interactions and processes. Positive ions directed along the dielectric channel can penetrate through the material, passing through its structure. Passage can occur through open pores and channels or through the matrix of the material itself. During the passage, ions can collide with atoms and molecules of the channel material, leading to scattering. Scattering and collisions can alter the trajectories and energies of the ions. As a result of these interactions, ions can change their direction of motion or lose energy. This can involve electron ionization, excitation of electrons, or other energy transfer processes. Positive ions can interact with negatively charged groups within the channel material, resulting in electrostatic interactions. This charge exchange interaction can influence the trajectory and energy of the ions. In work (Clark Turner et al. 1995) stopping cross section for protons and deuterons in aluminum oxide foils were studied at 0.9 – 2.5 MeV energy region. Thompson (1997) showed the presence of pores changes the energy loss during the transition of particles through the sample but allows to appear a guiding effect by the required pore configuration. In (Komarov et al. 2011) considered the transition of a proton beam with energy from 150 to 320 keV through tapered glass capillaries. Was shown that when beam passes through capillary, the angular width of the initial beam remains almost unchanged. For this case, the transmittance of the target was 10^{-3}. In (Razpet et al. 2004) by means of RBS was shown that maximum transmission of 2MeV He^+ ions through thick membranes varied from 30% to 65% which is comparable to the relative surface area covered by pores. It was shown that the effective atomic

surface density of investigated material is about 4-5 times lower than for bulk Al_2O_3. To evaluate the influence of the charge state and the effects of charge exchange of the incident ion on guiding, in several works, ions were used in the multiply charged state. By means of Ne^{6+} irradiation of alumina capillary angular distribution of ions has been determined by Juhász et al. (2009). Clear guiding effect has been found for 3 and 6 keV ion energies. An important detail was observing of photons originated from the tilted capillaries. Additionally, authors (Rehn et al. 2003, Reddy et al. 2019) have been considered that the low divergence of the beam at the exit from the membrane makes nanoporous alumina a promising material for use as masks for nanolithography.

Studying the transmission of positive ions through dielectric channels and understanding the existing problems are important aspects for optimizing processes and developing new applications related to ion processing and nanostructuring of materials. Table 1 presents a systematization of the main existing problems and ways to solve them.

Table 1. The main existing problems of the positive ion transmission through porous membrane and ways to solve them.

Problem	Description	Solution
Surface interactions	Positive ions interacting with the channel surface, leading to effects like ion absorption or adsorption.	- Use of surface coatings or protective layers.
Influence of channel size and shape	Impact of channel dimensions on ion passage, scattering, and energy loss.	- Optimization of channel dimensions for desired ion behavior. - Fabrication of channels with controlled size and shape.
Interaction with pores	Interactions between ions and pores within the channel, affecting ion trajectories and scattering.	- Surface functionalization to reduce ion-pore interactions.
Energy dependence	Variations in ion behavior with different energy levels.	- Precise control of ion energy during experiments. - Comparative analysis of ion behavior at different energy ranges.
Consideration of multiple scattering	Complex ion trajectories due to multiple collisions within the channel.	- Advanced modeling and simulation techniques to analyze multiple scattering effects. - Statistical analysis of ion trajectories.

In presented work the technique for nanopore alumina oxide matrix fabrication using different electrolytes is given and the optical properties of obtained samples, including transmission by means of RBS technique, are investigated. The dependence of ions transition through the matrix on the angle of the beam incidence on the sample is considered. The advantages of conducting research on the transmission and scattering of accelerated He+ ions in porous alumina channels include:

1. Understanding ion-material interactions: The research provides a deep understanding of the interaction between accelerated He+ ions and materials, particularly porous alumina. This is crucial for developing new materials and improving processes related to ion processing and nanoscale structuring.
2. Optimization of ion irradiation processes: Studying the transmission and scattering of He+ ions in porous alumina helps optimize the conditions of ion irradiation, including energy selection,

incident angle, and other parameters. This can lead to improved outcomes in material processing and the creation of structures with desired properties.

2. Materials and Methods

2.1. Production of Porous Alumina Membranes

Matrices of dielectric channels based on porous anodic alumina (PAA) were formed by electrochemical anodizing. Aluminum foil with the thickness 150 μm was used as a substrate. Studies (Muratova et al. 2013, Muratova et al.2017) have shown the geometric dimensions of pores depend on technological conditions of membrane formation in a wide range. Pore diameters can vary from nanometers to micrometers. Muratova et al. (2013) investigated how variable technological parameters (electrolyte composition, voltage, etc.) can affect to the structures. In our study the used conditional parameters are presented in Table 2.

Table 2. Technological parameters of electrochemical anodizing of aluminum foil.

| Sample title	Stage	Etching process	Electrolyte type and concentration (vol. %)	Glycerol [vol.%]	Voltage [V]	Process temperature [°C]	Process time, min
PAA_S	1	Electrochem.	H_2SO_4 (30)	15	20	5	3
	2	Chemical	H_2CrO_4 (7)	–	–	20	3
	3	Electrochem.	H_2SO_4 (30)	15	25	5	1
	4	Chemical	H_2CrO_4 (7)	–	–	20	3
	5	Electrochem.	H_2SO_4 (30)	15	25	5	123
PAA_P	1	Electrochem.	H_3PO_4 (10)	15	110	3	20

For the formation of highly ordered porous alumina with a pore diameter of ≈20 nm additional stages of chemical pre-structuring of aluminum foil are required. At the first stage of anodizing, pores are generated in energetically advantageous places, then the upper sacrificial layer is etched away, and nuclei remain on the surface for subsequent pore formation. The introduction of such stages makes it possible to obtain a porous structure as a close-packed ordered structure. As was shown in (Stępniowski et al. 2014), a viscosity plays significant role in a structural formation. So, the glycerol was used to raise the viscosity of solvents in the etching process.

2.2. Helium İons Transition through Alumina Membrane

To study (Shemukhin et al. 2017, Shemukhin and Muratova 2014, Luchinin et al. 2015, Zhilenkov et al. 2020) the transition of an ion beam through dielectric channels, a facility based on the AN-2500 accelerator, located at the SINP MSU was used. The accelerator based on Van de Graaff system is capable of accelerating particles (protons and He+ ions) to an energy of 2.5 MeV. For convenience of operations inside the accelerator's vacuum chamber all the membranes were fixed using a fluoroplastic disk frame (Figure 1). This made it possible to avoid specimen deformation during testing.
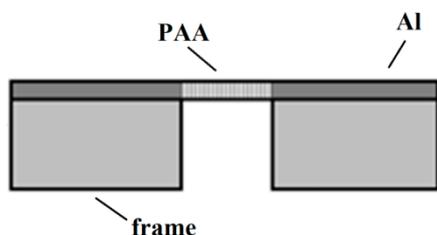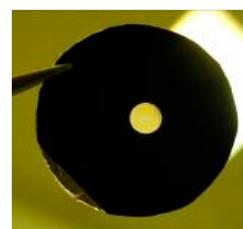
(a)   (b)

Figure 1. Schematic image (a) and photograph (b) of the frame for the PAA membrane.

A special experimental chamber was created, including collimating diaphragms, a beam monitoring system, a back-scattered ion detection system, and a goniometric system. A collimated beam of 1.2 MeV He$^+$ ions enter the membrane: one part of the beam passes through the capillaries and the current is recorded using a Faraday cup, while the other part is scattered and recorded using a semiconductor detector. In all experiments, the detected scattering angle was 120°. The diameter of the beam on the membrane was about 1 mm. The residual pressure in the chamber did not exceed $5*10^{-4}$ Pa. The current density on the target was kept constant at 4 nA.

3. Results and Discussion

3.1. Structural Characterization

3.1.1. SEM Measurements

The structure of the obtained membranes was examined using a scanning electron microscope (SEM). Examples of the surface structure of membranes obtained in various electrolytes are shown in Figure 2.
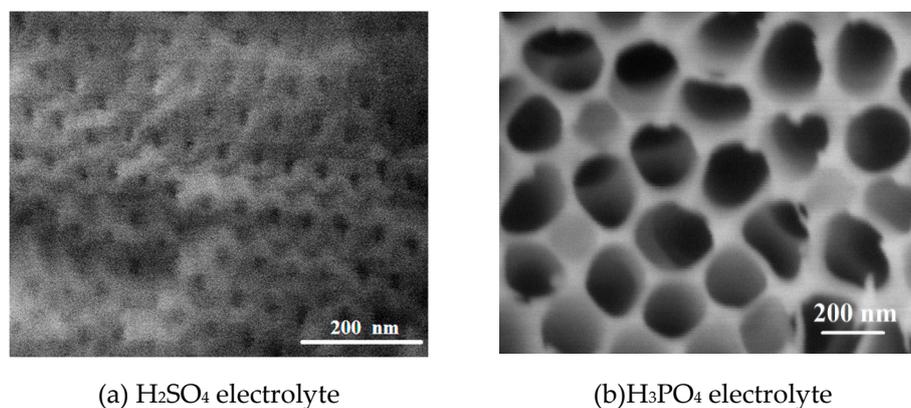

(a) H$_2$SO$_4$ electrolyte   (b)H$_3$PO$_4$ electrolyte

Figure 2. SEM images of the surface of membranes PAA obtained in different electrolytes.

Two series of obtained membranes have pores with significantly different diameter sizes (Figure 2). When using the electrolyte based on H$_2$SO$_4$, membranes with a thickness of about 10 μm are formed, with an average pore diameter of 20 nm, a barrier layer thickness of ≈ 200 nm, and their pore concentration is 350 pieces/μm^2. On the other hand, the geometrical parameters of the membranes obtained in the H$_3$PO$_4$-based electrolyte are as follows: an average pore diameter of 80 nm, a porous layer thickness of 10 μm, a barrier layer thickness of ≈ 200 nm, a pore concentration of 50 pieces/μm^2. In all the resulting membranes there is a barrier layer - the bottom of the pore - a layer of dense alumina separating the porous layer from the substrate (Figure 3).
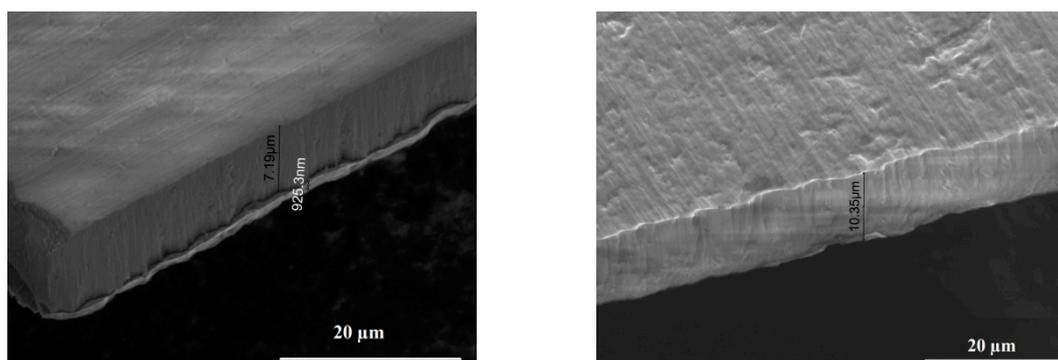
(a) with the barrier layer   (b) without the barrier layer

Figure 3. SEM images of cross-section of PAA_S membranes before and after removal of the barrier layer.

The presence of a barrier layer greatly affects the transmittance in experiments on the interaction of membranes with ion beams. In this case, the transmittance is the ratio of the intensity of the transmitted beam of helium ions to the incident beam. The difference in transmittance with and without a barrier layer can differ tenfold. Taking this important point into account, the removal of the barrier layer was carried out by chemical etching of the back side of the membrane in concentrated hydrochloric acid (HCl) for 10 minutes.

3.1.2. Fractal Dimension Evaluation

Surface topography is usually described in terms of surface roughness. Surface roughness is solely a function of height, that is, information about lateral topography is lost. Studies (Ponomareva et al. 2012, Ponomareva et al. 2013, Alattas et al. 2022) have shown that fractal dimension parameters allow to show more accurately the depending on sample structural features in dependence on different factors, such as fabrication conditions, treatment procedures, material compositions and so on.

Here fractal dimension was estimated from SEM images using cube counting, triangulation and power spectra density methods. Results are shown in Table 3.

Table 3. Fractal dimension of obtained PAA samples.

Sample title	Cube counting	Triangulation	PSD
PAA_S	2.60	2.64	2.70
PAA_P	2.47	2.54	2.39

3.2. Optical Properties

3.2.1. He$^+$ Ion Beam Transmission Measurements

The results of the ion beam transmission through membranes obtained in an electrolyte based on H_3PO_4 are demonstrated at Figure 4a. A small part of the ion beam passes through a porous matrix. Transmittance of 0.15 was registered by means of current measurement device, a significant current drop was observed when the membrane deviates from the normal by 1.5 degrees.
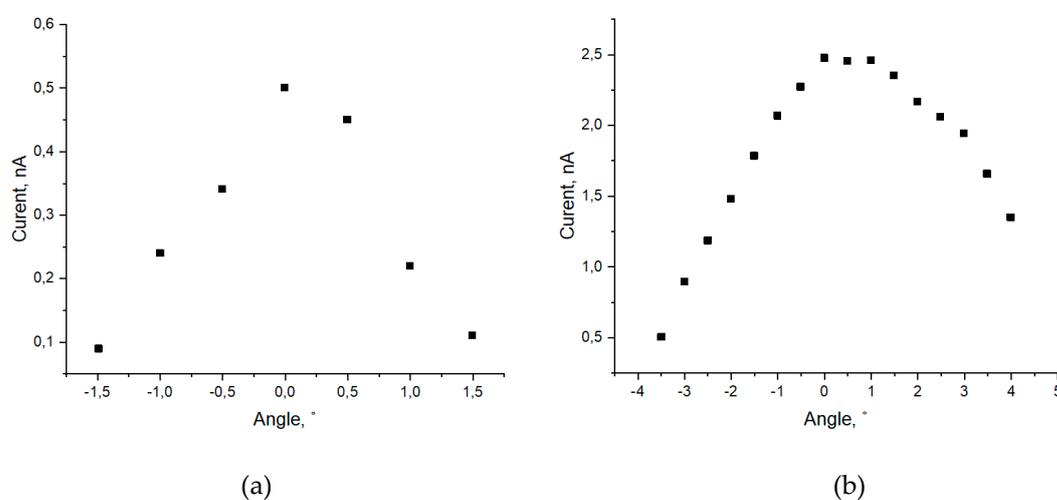

(a)   (b)

Figure 4. Dependence of the He$^+$ ions number passing through membranes on the angle of inclination. Membranes obtained in electrolytes based on H_3PO_4(a) and H_2SO_4 (b).

At the same time, the results of accelerated beams transition through membranes prepared in an electrolyte based on H_2SO_4 (Figure 4b) showed that the intensity of transmitted beam practically does not change within 2.5 degrees. The reducing of the signal in two times corresponds to the rotation of the target by 3 degrees. Measured transmittance was in range 0.50-0.625, depending on the sample thickness.

When we register number of transmitted ions by a Faraday cup, we do not take into account secondary electrons emitted from the pores surface. They can cause an error in the study of the angular distributions and the number of transmitted ions. To exclude secondary electron contribution, a sample consisting of a 20 nm HfO_2 film on a monocrystalline silicon substrate was installed behind a porous alumina membrane. Comparing the statistics in the maximum of the distribution of backscattered particles (Figure 5), the number of high-energy particles passed is ≈ 0.6 of the initial beam current like shown as well on Figure 4. However, with a deviation of 1.5 degrees, the current of the transmitted particles decreases at 4 times, in comparing with the orientation relative to the beam axis (Figure 5). Herewith, up to half of the charged particles passed through membrane in accordance with current device. At the same time, with a deviation of 3 degrees in the high-energy part of the spectrum there are practically no backscattered particles from Hf, and in the case of registration with a current device 25% of the beam passes. This suggests that with a small angular scattering on the membrane wall a sufficiently large number of electrons are generated, which must be considered when further using of such membranes.
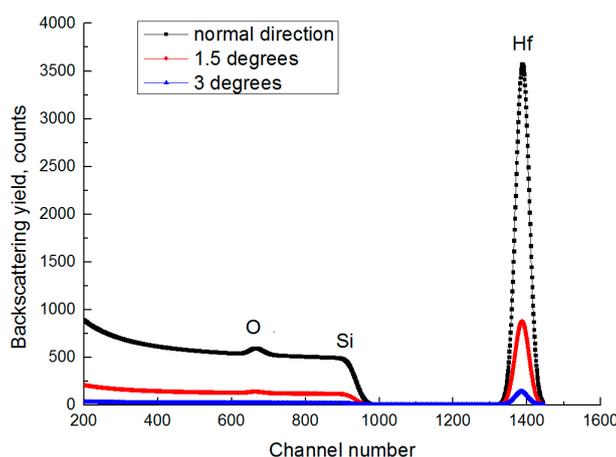

Figure 5. Energy spectrum of backscattered He⁺ ions with an energy of 1200 keV. The black curve is the spectrum along the normal direction, the red curve is the spectrum when the deviation is 1.5 degrees from the normal, the blue curve is the spectrum when the deviation is 3 degrees.

The beam energy resolution was estimated using SIMNRA simulation of the slope of the signal obtained by scattering helium ions from the layer of hafnium dioxide. Balakshin et al. (2018) shown that the resolution of the used spectrometry path is 15 keV. The energy resolution of the RBS technique with the use of a porous alumina membrane worsened and amounted to about 40 keV.

When studying using the Energy-dispersive X-ray spectroscopy (EDS) and RBS methods, there were no significant differences in the composition and stoichiometry of the membranes obtained in electrolytes based on H_2SO_4 and H_3PO_4.

3.2.2. Ultraviolet-Visible Spectroscopy (UV-Vis)

The authors (Muratova and Matyushkin 2014, Matyushkin et al. 2014, Matyushkin et al. 2017, Tian et al. 2021) of the work carried out studies of optical properties of PAA membranes, (Figure 6) in the visible wavelength range, in order to analyse the width of the energy gap. According to the transmission spectra, it is possible to calculate the energy gaps for PAA membranes with different pore diameters using the formula (Eq. (1)):

$$E = \frac{h \cdot c}{\lambda}, \qquad\qquad (1)$$

where h – Planck's constant, c – light speed, λ - critical wavelength, at which increase of light transmission begins. The results of the calculations are presented in Table 3.

Table 3. Energy gap of Al_2O_3 membranes with different pore diameters.

Composition	Average pore diameter[nm]	λ_c[nm]	Energy gap [eV]
PAA_S	20–30	≈ 200	6,2
PAA_P	180–220	≈ 700	1,77

The decrease in the band gap in the work is explained by the presence of oxygen vacancies near the valence band (alumina is characterized by an oxygen deficiency). The presence of oxygen vacancies leads to the appearance of localization centers for both electrons and holes, and, consequently, to the splitting of energy levels. If to compare two electrolytes, then when using the phosphoric acid PO_4^{3-}–anions, embedded in the structure, release $3H^+$, while when embedding anions of sulfuric acid SO_4^{2-} stands out $2H^+$. Free hydrogen ions tend to form a bond with oxygen to form water. Consequently, in the first case, more oxygen ions are required and, as a result, more oxygen vacancies are formed in the structure, which leads to the formation of additional levels in the forbidden zone. All this leads to the fact that the formed porous layer in the electrolyte based on H_2SO_4 has fewer localized levels and, consequently, a larger energy gap (≈ 6 eV) than based on H_3PO_4 (≈ 2 eV).

Thus, the valence band of the porous layer based on H_2SO_4 is completely filled with electrons and separated from the free zone following it by a wide energy gap. This structure corresponds to dielectrics that are characterized by a fully valence band filled with electrons and a completely free conduction band. If there is no thermal excitation of electrons to conduction band levels, then such materials behave like insulators. With our experimental parameters (the beam current in all experiments did not exceed 15 nA), this condition was always fulfilled. In this case, according to experimental data, a much larger number of ions pass through the membrane based on H_2SO_4. Thus, the mechanism of ions transition through the membrane is associated not only with small angular scattering, but also, probably, with the effect of charging the pore walls.

4. Conclusions

We have studied porous anodic aluminium oxide membranes with a system of ordered nanoscale (pore diameter of 20 nm and more) capillaries with an aspect ratio of up to five hundred. It was shown that the transmittance of high-energy ion beams for membranes made based on H_2SO_4 is significantly greater than based on H_3PO_4. It could be explained by structural differences. Membrane fabricated using H_2SO_4 has a higher pore concentration as well as a higher fractal dimension.

Based on a study of the transmission spectra, the choice of the membrane's type for studying the transmission of accelerated beams through the membranes was made in favour of those that were formed in the electrolyte based on H_2SO_4. Nanoporous alumina-based membranes were used successfully to provide the transporting of a flux of high-energy helium ions: for membranes with a pore diameter of 20 nm, the transmittances are in the range of 0.50-0.625.

References

Ahmad, N., Javed, M., Qamar, M. A., Kiran, U., Shahid, S., Akbar, M. B., Sher M. and Amjad A. (2022), "Synthesis, characterization and potential applications of Ag@ZnO nanocomposites with S@g-C_3N_4", *Adv. in Mater. Res.* **11 (3)**, 225-235. https://doi.org/10.12989/amr.2022.11.3.225.

Saad, M., Hadji, L. and Tounsi, A. (2021) "Effect of porosity on the free vibration analysis of various functionally graded sandwich plates" *Adv. in Mater. Res.* **10 (4)**, 293-311. https://doi.org/10.12989/amr.2021.10.4.293.

Hamad, L. B., Khalaf, B. S. and Faleh, N. M. (2019) "Analysis of static and dynamic characteristics of strain gradient shell structures made of porous nano-crystalline materials", *Adv. in Mater. Res.* **8 (3)**, 179-196. https://doi.org/10.12989/amr.2019.8.3.179.

Stolterfoht, N., Yamazaki, Y. (2016), "Guiding of charged particles through capillaries in insulating materials", *Phys. Rep.*, **629**, 1–107. https://doi.org/10.1016/j.physrep.2016.02.008.

Borka, D., Borka Jovanović, V., Lemell, C. and Tőkési, K. (2017), "Electron transmission through a macroscopic platinum capillary", *Nucl. Instruments Methods Phys. Res. Sect. B Beam Interact. with Mater. Atoms.*, **406,** 413–416. https://doi.org/10.1016/J.NIMB.2017.02.024.

Pinilla, S., Campo, T., Sanz, J.M., Márquez, F. and Morant, C. (2019), "Highly ordered metal-coated alumina membranes: Synthesis and RBS characterization", *Surf. Coatings Technol.*, **377**, 124883. https://doi.org/10.1016/J.SURFCOAT.2019.08.012.

Su, T., He, L., Mo, R., Zhou, C., Wang, Z., Wang, Y., Hong, P., Sun, S. and Li, C. (2018), "A non-enzymatic uric acid sensor utilizing ion channels in the barrier layer of a porous anodic alumina membrane", *Electrochem. Commun.*, **96**, 113–118. https://doi.org/10.1016/J.ELECOM.2018.10.017.

Costa, C.M., Lee, Y.-H., Kim, J.-H., Lee, S.-Y. and Lanceros-Méndez, S. (2019), "Recent advances on separator membranes for lithium-ion battery applications: From porous membranes to solid electrolytes", *Energy Storage Mater.*, **22**, 346–375. https://doi.org/10.1016/J.ENSM.2019.07.024.

Liu, G., Li, K., Zhang, Y., Du, J., Ghafoor, S. and Lu, Y. (2020), "A facile periodic porous Au nanoparticle array with high-density and built-in hotspots for SERS analysis", *Appl. Surf. Sci.*, **527**, 146807. https://doi.org/10.1016/J.APSUSC.2020.146807.

Evseev, A.P., Kozhemiako, A.V., Kargina, Y.V., Balakshin, Y.V., Zvereva, E.A., Chernysh, V.S., Gongalsky, M.B. and Shemukhin, A.A. (2020) ,"Radiation-induced paramagnetic defects in porous silicon under He and Ar ion irradiation", *Radiat. Phys. Chem.*, **176**, 109061. https://doi.org/10.1016/j.radphyschem.2020.109061.

Bensaid, I., and Bekhadda, A. (2018) "Thermal stability analysis of temperature dependent inhomogeneous size-dependent nano-scale beams", *Adv. in Mater. Res.* **7 (1)**, 1-16. https://doi.org/10.12989/amr.2018.7.1.001.

Abdel-Zaher, N. A., Moselhey M.T.H. and Guirguis O. W. (2017) "Ultraviolet-ozone irradiation of HPMC thin films: Structural and thermal properties", *Adv. in Mater. Res.* **6(1)**, 001-12. https://doi.org/10.12989/amr.2017.6.1.001.

Alattas, K.A.; Mostafaee, J.; Alanazi, A.K.; Mobayen, S.; Vu, M.T.; Zhilenkov, A.; Abo-Dief, H.M. Nonsingular Terminal Sliding Mode Control Based on Adaptive Barrier Function for nth-Order Perturbed Nonlinear Systems. Mathematics 2022, 10, 43. https://doi.org/10.3390/math10010043.

Stolterfoht, N., Bremer, J.-H., Hoffmann, V., Hellhammer, R., Fink, D., Petrov, A. and Sulik, B.(2002), "Transmission of 3 keV Ne^{7+} Ions through Nanocapillaries Etched in Polymer Foils: Evidence for Capillary Guiding", *Phys. Rev. Lett.*, **88**, 133201. https://doi.org/10.1103/PhysRevLett.88.133201.

Du, G., Guo, J., Wu, R., Guo, N., Liu, W., Ye, F., Sheng, L., Li, Q. and Li, H. (2015), "The first interdisciplinary experiments at the IMP high energy microbeam", *Nucl. Instruments Methods Phys. Res. Sect. B Beam Interact. with Mater. Atoms.*, **348**, 18–22https://doi.org/10.1016/J.NIMB.2015.01.066.

Fujita, N., Ishii, K. and Ogawa, H. (2011), "Development of two-dimensional mapping technique by in-air-PIXE with metal capillary", *Nucl. Instruments Methods Phys. Res. Sect. B Beam Interact. with Mater. Atoms.*, 269, 1023–1025. https://doi.org/10.1016/j.nimb.2010.11.065.

Folkard, M., Prise, K.M., Grime, G., Kirkby, K. and Vojnovic, B. (2009), "The use of microbeams to investigate radiation damage in living cells", *Appl. Radiat. Isot.*, **67**, 436–439. https://doi.org/10.1016/j.apradiso.2008.06.015.

Grotzer, M.A.,Schültke, E., Bräuer-Krisch, E. and Laissue, J.A. (2015), "Microbeam radiation therapy: Clinical perspectives", *Phys. Medica.*, **31**, 564–567. https://doi.org/10.1016/j.ejmp.2015.02.011.

Michelet, C., Moretto, P. (1999), "3D mapping of individual cells using a proton microbeam", *Nucl. Instruments Methods Phys. Res. Sect. B Beam Interact. with Mater. Atoms.*, **150**, 173–178. https://doi.org/10.1016/S0168-583X(98)01015-5.

Feng, S., Ji, W. (2021) "Advanced nanoporous anodic alumina-based optical sensors for biomedical applications", *Frontiers in Nanotechnology*, **3**, 678275. https://doi.org/10.3389/fnano.2021.678275

Domagalski, J.T., Xifre-Perez, E. and Marsal, L.F. (2021) "Recent Advances in Nanoporous Anodic Alumina: Principles, Engineering, and Applications", *Nanomaterials*, **11**(2), 430. https://doi.org/10.3390/nano11020430

Ruiz-Clavijo, A., Caballero-Calero, O. and Martín-González, M., (2021) "Revisiting anodic alumina templates: from fabrication to applications", *Nanoscale*, **13**(4), 2227-2265. https://doi.org/10.1039/d0nr07582e

Davoodi, E., Zhianmanesh, M., Montazerian, H., Milani, A.S. and Hoorfar, M. (2020), "Nano-porous anodic alumina: fundamentals and applications in tissue engineering", J *Mater Sci: Mater Med*, **31**, 60. https://doi.org/10.1007/s10856-020-06398-2

Alvarez-Carrizal, R. P., Rodríguez-García, J. A., Cortés-Hernández, D. A., Esparza-Vázquez S. J. and Rocha-Rangel E. (2021) "Manufacture of Al2O3/Ti composite by aluminum bonding reaction for their use as a biomaterial", *Adv. in Mater. Res.* **10 (4)**, 331-341. https://doi.org/10.12989/amr.2021.10.4.331.

Pandey, V. K., Patel, B. P. and Guruprasad S. (2016)"Mechanical properties of Al/Al2O3 and Al/B4C composites", *Adv. in Mater. Res.* **5 (4)**, 263-277. https://doi.org/10.12989/amr.2016.5.4.263.

Vokhmyanina, K.A., Zhukova, P.N., Irribarra, E.F., Kubankin, A.S., Le Thu Hoai, Nazhmudinov, R.M., Nasonov, N.N. and Pokhil, G.P. (2013), "Investigation of contactless electron transmission through dielectric channels", *J. Surf. Investig.*, **7**, 271–275. https://doi.org/10.1134/S1027451013020249

Zhang, H.Q., Akram, N. and Schuch, R. (2016), "Guiding and scattering of ions in transmission through mica nanocapillaries", *Phys. Rev. A*, **94**, 032704. https://doi.org/10.1103/PhysRevA.94.032704

Röding, M., Tomaszewski, P., Yu, Sh., Borg, M. and Rönnols, J. (2022), "Machine learning-accelerated small-angle X-ray scattering analysis of disordered two- and three-phase materials", *Frontiers in Materials*, **9**, 956839. https://doi.org/10.3389/fmats.2022.956839

Clark Turner, D., Mangelson, N.F. and Rees, L.B. (1995),"Determination of aluminum oxide stopping cross sections for protons and deuterons by backscattering from thin targets", *Nucl. Inst. Methods Phys. Res. B.*, **103**, 28–32. https://doi.org/10.1016/0168-583X(95)00562-5.

Thompson, G.E. (1997),"Porous anodic alumina: fabrication, characterization and applications", *Thin Solid Films*, **297**, 192–201.http://www.sciencedirect.com/science/article/pii/S0040609096094400.

Komarov, F.F., Kamyshan, A.S. and Grishin, P.A. (2011),"Peculiarities of proton transmission through tapered glass capillaries", *Nuovo Cim. Della Soc. Ital. DiFis. C.*, **34**, 365–372. https://doi.org/10.1393/ncc/i2011-10920-0.

Razpet, A., Possnert, G., Johansson, A., Hallén, A. and Hjort, K. (2004), "Ion transmission and characterization of ordered nanoporous alumina", Nucl. *Instruments Methods Phys. Res. Sect. B Beam Interact. with Mater. Atoms.*, **222**, 593–600. https://doi.org/10.1016/j.nimb.2004.03.072.

Juhász, Z.,Sulik, B., Biri, S.,Iván, I.,Tokési, K., Fekete, É.,Mátéfi-Tempfli, S.,Mátéfi-Tempfli, M., Víkor, G.,Takács, E., Pálinkás, J.(2009), "Ion guiding in alumina capillaries: MCP images of the transmitted ions", *Nucl. Instruments Methods Phys. Res. Sect. B Beam Interact. with Mater. Atoms.*, **267**, 321–325. https://doi.org/10.1016/j.nimb.2008.10.017.

Rehn, L.E., Kestel, B.J.,Baldo, P.M., Hiller, J., McCormick, A.W. and Birtcher, R.C. (2003), "Self-organized porous-alumina implantation masks for generating nanoscale arrays", *Nucl. Instruments Methods Phys. Res. Sect. B Beam Interact. with Mater. Atoms.*, **206**, 490–494. https://doi.org/10.1016/S0168-583X(03)00805-X.

Reddy, P.R., Ajith, K.M. and Udayashankar, N.K. (2019), "Structural and optical analysis of silver nanoparticles grown on porous anodic alumina membranes by electro-less deposition", *Mater. Today Proc.*, **19**, 2633–2638. https://doi.org/10.1016/J.MATPR.2019.10.109.

Muratova, E.N., Spivak, Y.M., Moshnikov, V.A., Petrov, D.V., Shemukhin, A.A. and Shimanova, V.V. (2013), "Influence of technological parameters of nanoporous Al2O3 layers' preparation on their structural characteristics", *Glas. Phys. Chem.*, **39**, 320–328. https://doi.org/10.1134/S1087659613030140.

Muratova, E.N.,Luchinin, V.V., Moshnikov, V.A.,Lifshits, V.A., Matyushkin, L.B., Panov, M.F., Potrakhov, N.N.,Galunin, S.A.,Ishin, V.V. and Shemukhin, A.A. (2017), "Features of the formation of nanoporous membranes based on alumina from foil and new fields of applications", *Glas. Phys. Chem.*, **43**, 163–169. https://doi.org/10.1134/S1087659617020122.

Stępniowski, W.J., Forbot, D., Norek, M., Michalska-Domańska, M. and Król, A. (2014), "The impact of viscosity of the electrolyte on the formation of nanoporous anodic aluminum oxide", *Electrochimica Acta*, **133**, 57-64. https://doi.org/10.1016/j.electacta.2014.04.039.

Shemukhin, A.A., Balaskshin, Y.V., Evseev, A.P. and Chernysh, V.S. (2017), "The parameter influences of ion irradiation on the distribution profile of the defect in silicon films", *Nucl. Instruments Methods Phys. Res. Sect. B Beam Interact. with Mater. Atoms.*, **406**, 507–510. https://doi.org/10.1016/j.nimb.2017.04.055.

Shemukhin, A.A., Muratova, E.N. (2014), "Investigation of transmission of 1.7-MeV He+ beams through porous alumina membranes", *Tech. Phys. Lett.*, **40**, 219–221. https://doi.org/10.1134/S1063785014030110.

Luchinin, V.V., Moshnikov, V.A., Muratova, E.N., and Samigullin, R.S. (2015), "Formation of ordered nanoscale capillary membranes based on anodic alumina", *J. Phys. Conf. Ser.*, **586**, 012008. https://doi.org/10.1088/1742-6596/586/1/012008.

Ponomareva, A.A., Moshnikov, V.A., Maraeva, E.V. and Suchaneck, G. (2012), "Fractal analysis of surfaces comprising hierarchical structures", *Proceedings ECCM15 of 15th European Conference on Composite Materials*, Venice, Italy, June.

Ponomareva, A.A., Moshnikov, V.A. and Suchaneck, G. (2013), "Mesoporous gas-sensitive SnO2-SiO2 nanocomposites. Handbook of Functional Nanomaterials V.2", Nova Science Publishers, Inc. New York, NY, USA.

Balakshin, Y.V., Shemukhin, A.A., Nazarov, A.V., Kozhemiako, A.V. and Chernysh, V.S. (2018), "In situ modification and analysis of the composition and crystal structure of a silicon target by ion-beam methods", *Tech. Phys.*, **63**, 1861–1867. https://doi.org/10.1134/s106378421812023x.

Muratova, E.N., Matyushkin, L.B. (2014), "Investigation of the optical properties of nanoporous membranes based on alumina", *Smart Nanocomposites*, **4**, 25–31.

Tian, M.-W.; Yan, S.-R.; Mohammadzadeh, A.; Tavoosi, J.; Mobayen, S.; Safdar, R.; Assawinchaichote, W.; Vu, M.T.; Zhilenkov, A. Stability of Interval Type-3 Fuzzy Controllers for Autonomous Vehicles. Mathematics 2021, 9, 2742. https://doi.org/10.3390/math9212742

Matyushkin, L.B., Muratova, E.N., Spivak, J.M., Shimanova, V.V., Korlyakova, S.A. and Moshnikov, V.A. (2014), "Optical transmission spectra of porous aluminamembranes with different pore size", *J. Phys. Conf. Ser.*, **572**, 012031.https://doi.org/10.1088/1742-6596/572/1/012031.

Matyushkin, L.B., Muratova, E.N. and Panov, M.F. (2017), "Determination of the alumina membrane geometrical parameters using its optical spectra", *Micro Nano Lett.*, **12**, 100–103. https://doi.org/10.1049/mnl.2016.0353.

Zhilenkov, Anton A. et al. 'Intelligent Autonomous Navigation System for UAV in Randomly Changing Environmental Conditions'. 1 Jan. 2020 : 6619 – 6625. https://doi.org/10.3233/JIFS-179741.